

# Characterization and Time Dependence of Amphotericin B: Deoxycholate Aggregation by Quasielastic Light Scattering

M. THERESA LAMY-FREUND\*, SHIRLEY SCHREIER<sup>‡</sup>, ROBERT M. PEITZSCH<sup>§</sup>, AND WAYNE F. REED<sup>§\*</sup>

Received January 22, 1990, from the \*Institute of Physics, Universidade de S. Paulo, C.P. 20516, S. Paulo, the <sup>‡</sup>Laboratory of Molecular Biophysics, Department of Biochemistry, Institute of Chemistry, Universidade de S. Paulo, C.P. 20780, CEP 01498, S. Paulo, Brazil, and the <sup>§</sup>Department of Physics, Tulane University, New Orleans, LA. Accepted for publication April 25, 1990.

**Abstract** □ Quasielastic light scattering measurements of amphotericin B (AB):deoxycholate (DOC) preparations provided information about particle size and aggregation as a function of concentration. The data allowed the time dependence of the aggregation to be followed and indicated that the initial rates of the change in average equivalent hydrodynamic diameter increased with decreasing concentration. The results extend the model proposed by Lamy-Freund and co-workers, which describes AB:DOC systems as consisting of AB:DOC mixed aggregates co-existing with pure DOC micelles. Although the AB:DOC aggregates are unstable at all concentrations studied, the rate of aggregation increases by three orders of magnitude as the concentration is reduced from 20 mM (DOC concentration) to the concentration region of DOC micellization. These results are in agreement with the different distribution of AB and DOC in the body of experimental animals, and may be of relevance for the understanding of the serious toxic effects of AB.

The polyene antibiotic amphotericin B (AB) is extensively used in the treatment of systemic mycotic infections, in spite of its serious toxic effects, such as hemolysis and nephrotoxicity.<sup>1</sup> Amphotericin B has been found to carry out its lytic action by modifying membrane permeability.<sup>2</sup> However, the mechanism of toxicity is still largely unknown.

Several studies have related the therapeutic and toxic effects of AB and other pharmacologically active compounds to the nature of aggregates formed by these compounds.<sup>3-6</sup> The toxicity of AB has been found to decrease considerably when the antibiotic is carried by a phospholipid<sup>7-10</sup> rather than by a bile salt, reinforcing the view that the nature of the aggregate plays an important role in the mechanism of toxicity. Thus, it is of interest to understand the organizational state of aggregates formed by AB under different conditions, as well as the effect of aggregation upon other properties of the antibiotic, such as chemical reactivity.

Due to the hydrophobicity of AB, pharmaceuticals currently use deoxycholate (DOC), as a carrier, because of its compatibility with the human body. However, AB:DOC aggregates suffer from self-aggregation, hence creating "super"-aggregates. This has been verified by differential ultrafiltration and by spectroscopic techniques such as UV absorption, circular dichroism, and light scattering and electron spin resonance (ESR).<sup>11-14</sup> (It has been pointed out that UV absorption and CD spectra are fairly insensitive to the degree of aggregation.) The time dependence of this self-aggregation process has been mentioned only briefly.<sup>12</sup>

We have previously examined the kinetics of AB autoxidation<sup>15</sup> and the role of aggregation in this process.<sup>16</sup> Amphotericin B autoxidation has been implied in the mechanism of the inactivation<sup>17,18</sup> of the drug and in its membrane lytic action, via oxidative damage.<sup>19,20</sup> In addition, we have examined the AB:DOC system (1:2 mol/mol, the clinically used preparation Fungizone) by ESR spectroscopy and found that

at high enough concentrations, the system consists of mixed AB:DOC aggregates coexisting with pure DOC micelles.<sup>14</sup>

Here we present time-dependent quasielastic light scattering (QELS) data on the same systems, which yield a method of measuring the flocculation rates of AB:DOC aggregates, and show how these rates increase with decreasing AB:DOC concentration. This behavior is discussed in terms of the micellization properties of DOC and the low solubility of AB:DOC complexes.

## Experimental Section

**Chemicals**—Fungizone (AB:DOC) was provided by Squibb Industria Quimica S.A., Sao Paulo, Brazil, and was stored at 5 °C. Sodium deoxycholate (DOC); lot #38F-0015) and 5-doxyol stearic acid (5-SASL) were obtained from Sigma and were used as received. Doubly distilled, deionized water was used throughout. Unless otherwise noted, AB:DOC samples were prepared immediately before using by adding distilled H<sub>2</sub>O to the Fungizone, hence creating a 20 mM DOC sample in 37 mM KH<sub>2</sub>PO<sub>4</sub>, 37 mM Na<sub>2</sub>HPO<sub>4</sub> (phosphate) buffer at 25 °C and pH 7.4. Dilutions were made by addition of phosphate buffer at the same pH. Measurements were started ( $t = 0$  in the figures) ~30 s after dilution of the original 20 mM sample.

**Light Scattering**—Dynamic and static light scattering measurements were made using a Coherent I-90 argon ion laser operated at 488 nm as the light source, and a Brookhaven BI-2030 instrument for autocorrelation of the scattered intensity signal. Details of the custom-built goniometer and control and analysis programs, including calibration against National Bureau of Standards molecular weight standards, are presented elsewhere.<sup>21,22</sup> For the experiments on the AB:DOC system, autocorrelation curves were taken consecutively at a fixed observation angle of 90°, using adjustable acquisition and dead times in order to measure aggregation kinetics, and the data for each kinetic run were stored in single files. There were typically 100 separate autocorrelation curves per run. Because the mass of the AB:DOC aggregates ( $>5 \times 10^6$ ) is so much larger than that of the DOC micelles ( $\sim 5 \times 10^3$ ), it is impossible to measure a portion of the autocorrelation function which would correspond to the micellar scattering, no matter what type of data analysis is used. Therefore, only a standard second-order cumulant analysis<sup>23</sup> was used for determining the z-average diffusion coefficient ( $D$ ). The polydispersity index ( $Q$ ) was calculated by eq 1:

$$Q = \frac{\mu_2}{\Gamma^2} \quad (1)$$

where  $\Gamma$  and  $\mu_2$  are, respectively, the first and second moments of the expansion of the logarithm of the electric field autocorrelation function. The data were then analyzed using linear regression to fit the initial velocity of the increases in diffusion coefficients and total light scattering intensity.

For convenience and ease of interpretation, the equivalent hydrodynamic diameter, given by the familiar Stokes-Einstein equation:

$$D_H = kT/3\pi\eta D, \quad (2)$$

is used in some of the graphs and discussions, although the aggregates do not seem to be spherical. This latter assertion is based on the strong depolarized component of the light scattered by AB:DOC aggregates. The depolarized signals were autocorrelated using high extinction prism polarizers placed vertically before the scattering sample and horizontally before the photodetector. The depolarized scattering autocorrelation decay time versus  $\sin^2(\theta/2)$  had a non-zero intercept, which is strong evidence of shape anisotropy.<sup>24</sup>

The time and concentration dependence of the AB:DOC systems rendered it impossible to make molecular weight and radius of gyration measurements by static light scattering extrapolation methods made on serial dilutions of an AB:DOC stock solution. Nonetheless, at separately prepared, fixed concentrations where the aggregation kinetics was slow, absolute Rayleigh ratios were determined over an angular range and, hence, the weight average molecular weight of the aggregates could be estimated.

The DOC micelles in phosphate buffer (pH 7.4) were studied by QELS and static light scattering as a function of DOC concentration and added NaCl. Determinations of the diffusion coefficient for DOC micelles were made by measuring the autocorrelation function over the angular range  $\theta = 30^\circ$  to  $60^\circ$ , and calculating the slope of the plot of the reciprocal autocorrelation decay time versus  $\sin^2(\theta/2)$ .<sup>21</sup>

The refractive index increment measurements were made on a Brice-Phoenix differential refractometer. All static, QELS, and refractive index increment determinations were carried out at 25 °C.

**Electron Spin Resonance (ESR) Measurements**—The desired amount of label in chloroform solution (1% in moles of AB when AB was present or DOC in pure DOC preparations) was dried by a stream of nitrogen and kept under reduced pressure for 2 h. The aqueous preparations were added and the sample was vortexed for 5 min.

The ESR spectra were obtained in a Bruker ER 200 spectrometer equipped with an Aspect 2000 computer that was used for spectral subtractions. The spectra were generally completed within 0.5 h of adding the aqueous solutions to the labeled solution. The ESR results subsequently reported will refer to time averages over this time scale.

Flat quartz cells for aqueous solutions came from James Scanlon, Costa Mesa, CA. Spectra were run at room temperature ( $22 \pm 2^\circ\text{C}$ ).

## Results

**Light Scattering Measurements of Amphotericin B:Deoxycholate (AB:DOC) Systems**—Figure 1A shows the time dependence of the equivalent hydrodynamic diameter ( $D_H$ ) of the AB:DOC aggregates at DOC concentrations of 20.0, 10.0, and 5.8 mM.<sup>25</sup> Initial  $D_H$  values for freshly mixed 20 mM stock solutions were found to be  $\sim 350$  Å. Figure 1B shows the time-dependent increase of the total scattered intensity at  $\theta = 90^\circ$  and of the polydispersity index (eq 1) for 5.8 mM DOC. The intensity increase is further evidence of the size increase of the aggregates, whereas the increasing value of  $Q$  indicates that the aggregate population is becoming more polydisperse in time.

The solid curve in Figure 2 shows the logarithm of the initial rate of increase of  $D_H$  of the AB:DOC aggregates, expressed in Å/min, versus the concentration ([DOC]). The aggregation rate increased from  $\sim 1$  Å/min at 20 mM DOC to  $\sim 1000$  Å/min at 3.2 mM DOC. The sharpest part of the increase occurred between 3.2 and 3.7 mM DOC. Below 3.2 mM, the aggregation was too fast for the current technique to monitor.

The aggregates eventually precipitated out at, and below, a DOC concentration of  $\sim 16$  mM on a time scale of 10 h. For 5 to 16 mM, the precipitate was gelatinous. For concentrations  $> 16$  mM, uniform gels formed on a slightly longer time scale. Centrifugation of samples at different concentrations (which had been allowed to stand for 10 weeks) yielded a slightly orange-tinged supernatant, whose measured  $dn/dc$  value (0.209 mL/g) showed that virtually all of the original DOC was present in it. Thus, the precipitate is thought to consist almost wholly of AB.

Molecular weights were estimated for the AB:DOC aggregates at several concentrations from the total scattered light at several angles. The values of the total scattered light had

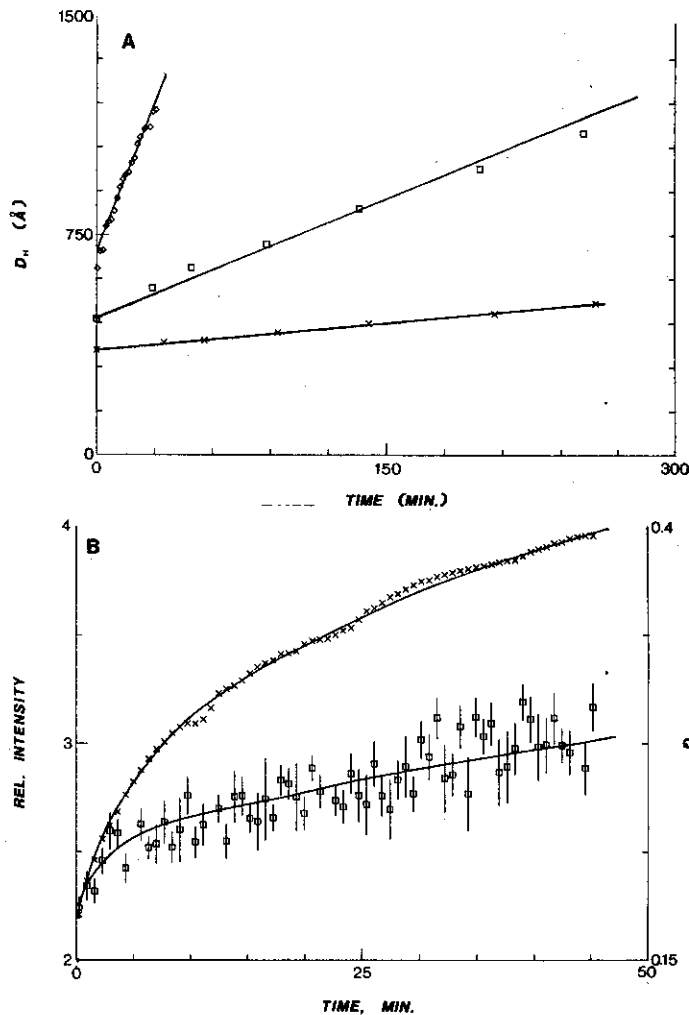


**Figure 1**—(A) Time dependence of AB:DOC aggregates average hydrodynamic diameter for the following DOC concentrations in pH 7.4 phosphate buffer: 20 mM (x); 10.0 mM (□); and 5.8 mM (◇). (B) Time dependence of relative scattered intensity at  $90^\circ$  (x) and polydispersity,  $Q$  (□) for 5.8 mM DOC under the same experimental conditions as in Figure 1A.

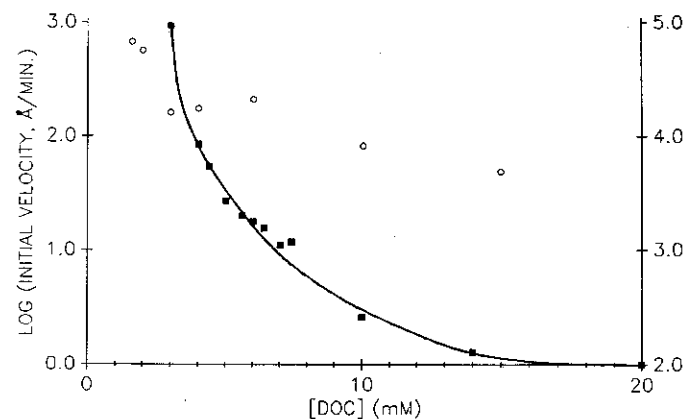


**Figure 2**—Initial rate of average hydrodynamic diameter change of AB:DOC mixed aggregates as a function of DOC concentration for no salt (■; scale on left) and 83 mM NaCl (○; scale on right).

to be corrected for a small absorbance at 488 nm. The procedure assumed a negligibly small second virial coefficient in the polynomial expansion for the osmotic pressure, and

used the absolute Rayleigh ratio divided by the concentration times the optical constant<sup>26</sup> of the system as the estimated molecular weight. The initial molecular weight of the AB:DOC aggregates at DOC concentrations between 12 and 20 mM was  $\sim 5 \times 10^6$  Da. These values are in rough agreement with Rinnert et al.<sup>11</sup> who measured molecular weights for AB:DOC aggregates in hydroalcoholic solution.

The apparent virial coefficient obtained by serial dilutions is a very large positive number, but is due to irreversible aggregation as a function of decreasing concentration and not to interaggregate repulsions. Direct concentration extrapolations made on serial dilutions yield meaningless results (i.e., negative intercepts on the plot of reciprocal Rayleigh scattering ratio times solute concentration versus concentration).

Attempts to perform similar experiments at higher ionic strength (83 mM NaCl:phosphate buffer, 300 mosM) led to faster aggregation kinetics and larger aggregates than in the case of no added NaCl. Initial diameters for 20 mM were  $\sim 1.5$   $\mu$ m. The turbidity of such aggregating solutions became high so quickly, in fact, that there was a significant amount of multiple scattering and only a few data points could be taken in these systems. Qualitatively, however, the overall pattern of aggregation as a function of concentration was the same as found at lower ionic strength. The unconnected points in Figure 2 (note that the scale on the right of the graph corresponds to these points) shows the logarithm of the rough initial velocities for AB:DOC in the NaCl:phosphate buffer.

**Light Scattering Measurements of Deoxycholate (DOC) Solutions**—Figure 3 shows  $D$  and  $D_H$  for DOC micelles versus DOC concentration in buffer at pH 7.4 in the absence of added NaCl. The increase in the diffusion coefficient between 4 and 6 mM DOC suggests that the actual size of the DOC micelle is concentration dependent. Apparently, a plateau in the diffusion coefficient is reached at  $\sim 4$  mM DOC, below which the scatter in the data reflects the increasing difficulty of autocorrelating very weak scattering signals. Below  $\sim 3$  mM, it was not possible to autocorrelate the scattered signal.

The ESR data (not shown) indicate that significant changes in the percentage of bound probe start to occur at  $\sim 3.5$  mM DOC. The changes observed with light scattering and with ESR correspond well with the reported stepwise changes in aggregation number in the process of bile salt micellization.<sup>27</sup>

As pointed out by Carey,<sup>28</sup> self-aggregation continues to occur below the 'effective critical micelle concentration' of bile salts. Therefore, we will refer to a concentration region of micelle formation (CRM). The CRM is shifted to lower values with increasing NaCl, as expected, and is in agreement with

previous ESR results.<sup>14</sup>

Total scattering intensity measurements showed that the aggregation number of the DOC micelles was dependent on DOC and salt concentrations. The aggregation numbers varied from 4 to 11 going from 2.5 to 10 mM DOC with no added salt. In the NaCl:phosphate buffer at pH 7.4, the aggregation number ranged from 4.3 at 2.4 mM DOC to 7.5 at 3.3 mM DOC, with gels forming above this latter concentration. Overall, these scattering results on pure DOC micelles are in agreement with the trends reported in the literature.<sup>29-32</sup>

**Electron Spin Resonance (ESR) Measurements**—The ESR spectra of 5-SASL incorporated in AB:DOC systems yielded results essentially identical to those obtained previously at high ionic strength.<sup>14</sup> Above 8 mM DOC, a composite spectrum was observed consisting of one component due to strongly immobilized probe and another due to weakly immobilized probe. By decreasing the concentration, the spectrum due to weakly immobilized probe progressively disappeared.

A comparison between these spectra and those of 5-SASL in pure DOC micelles showed that the component due to strongly immobilized probe corresponds to AB:DOC mixed aggregate, while that due to weakly immobilized probe refers to pure DOC micelles. Spectral subtractions yielded the percentages of each population and an analysis based on the model described by Lamy-Freund et al.<sup>14</sup> showed that at concentrations  $>8$  mM, the DOC:AB molar ratio in the mixed aggregates is  $\sim 1.3$  (Table I), the remaining DOC being present as micelles and monomers. This ratio decreases with increasing dilution. As the system is diluted below the CRM for DOC, the pure DOC micelles disappear and the DOC:AB molar ratio decreases further (Table I).

## Discussion

The literature concerning the self-aggregation of AB and other polyene antibiotics is fairly scarce and not much is known about the nature or time dependence of the aggregates. A previous report did not take into account the participation of DOC in the aggregates.<sup>12</sup>

Lamy-Freund et al., based on ESR spin labeling data, proposed a model for the AB:DOC (1:2, mol:mol) system, where mixed aggregates coexist with pure micelles above the CRM of DOC.<sup>14</sup> The DOC:AB mole ratio in the mixed aggregates decreases continuously and DOC is still present for the lowest AB concentration examined (1 mM AB). Filtration and centrifugation experiments provided indications for a concomitant increase in particle size. The present light scattering and ESR experiments are in basic agreement with the above model.

The increase in aggregation rate of the AB:DOC system versus [DOC] (Figure 2) appears to be closely correlated with

**Table I—Analysis of the Amphotericin B:Deoxycholate (AB:DOC) System from Electron Spin Resonance (ESR) Data as a Function of Dilution**

[AB], mM	Total [DOC]	[Micellar + Monomeric DOC], mM	[DOC in Mixed Aggregate], mM	DOC:AB Mole Ratio in Mixed Aggregates
10.0	20.0	7.0	13.0	1.3
5.0	10.0	3.5	6.5	1.3
4.0	8.0	2.8	5.2	1.3
3.0	6.0	2.7	3.3	1.1
2.5	5.0	2.4	2.6	1.0
2.2	4.4	2.1	2.3	1.0
2.0	4.0	1.9	2.1	1.0
1.7	3.4	1.9	1.5	0.9
1.5	3.0	1.7	1.3	0.9

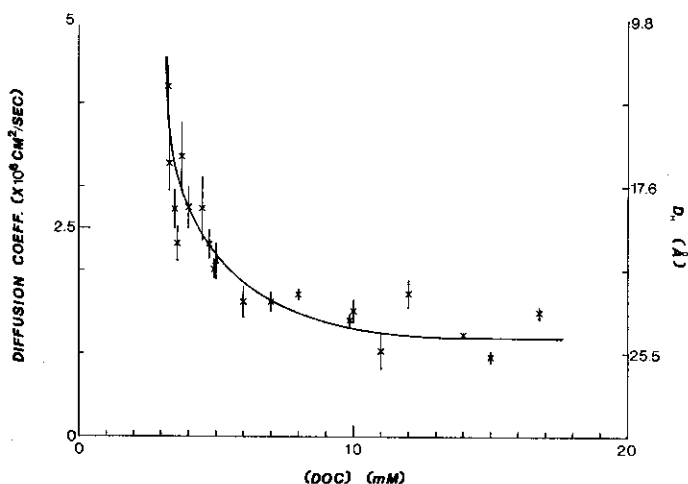


**Figure 3**—Diffusion coefficient and  $D_H$  of DOC versus [DOC] for the same conditions as in Figure 1.

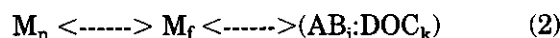
*D* versus [DOC] for pure DOC micelles (Figure 3). The aggregates become radically unstable as the CRM of DOC is approached. Pure DOC micelles have very low aggregation numbers (~4-11), so that the AB:DOC aggregates cannot be anything resembling AB neatly solubilized in DOC micelles. In fact, the ESR data show that DOC micelles coexist with the aggregates even in the CRM of DOC.

The time dependence of the parameters in Figures 1A and 1B are not susceptible to simple quantitative analysis. Since the particle size distribution of the aggregates is governed by a series of rate equations involving sums of pairwise aggregation steps and second-order rate constants, the number of adjustable parameters involved in even a simplified kinetic model would necessarily lead to a deceptively good fit to the data. Nevertheless, the initial rate of increase of the hydrodynamic diameter of the aggregates proved to be an effective parameter in characterizing the aggregation process (Figure 2).

The initial velocities presented in Figure 2 seem unusual at first glance. In general, the maximum aggregation rate would be expected to occur when all aggregate-aggregate encounters result in the two particles sticking together (i.e., when the process is purely diffusion limited). In a diffusion-controlled process, the aggregation rate should decrease with decreasing concentration. Figure 2 shows the opposite, namely that aggregation rate increases with decreasing concentration for the AB:DOC system. This suggests that it is the actual probability of two aggregates sticking together that is controlled by the concentration.

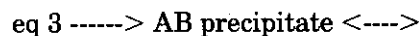
The ESR results indicating that the initial DOC:AB molar ratio of mixed AB:DOC aggregates decreases with decreasing concentration support this latter idea. Since pure AB is practically insoluble, the ratio DOC:AB should be directly related to the solubility of the aggregate and hence to the probability that two aggregates stick together when they encounter each other. Because the complete AB:DOC system is not initially in equilibrium under any of the conditions studied, it is not possible to establish true equilibrium equations between DOC monomers, DOC micelles, and AB:DOC aggregates. Since the final equilibrium state consists of precipitated AB, DOC micelles in equilibrium with monomer, and a trace of AB in solution at its very low solubility limit, the rate at which equilibrium is approached is governed by the rate at which the AB:DOC aggregates flocculate, which is in turn governed principally by the DOC:AB molar ratio (solubility) in the aggregates.

In this interpretation, the entire process can be summarized as follows. Upon dissolving the AB:DOC crystals, the DOC is dispersed into monomers, micelles, and aggregates with AB. The AB:DOC aggregates are unstable at any initial concentration. The source of the instability of the system is the low solubility of AB even when in AB:DOC aggregates. The DOC, nonetheless, tends towards equilibrium in the solution, partitioning itself between monomeric, micelle, and aggregate phases. The system would be in a semi-equilibrium of the following form:



where the equilibrium constants would depend on the relative free energy of DOC monomers being in the hydrophobic micellar and aggregate phases. In eq 3,  $M_n$  represents deoxycholate micelles of average aggregation number  $n$ ,  $M_f$  represents free deoxycholate monomers in solution, and  $(AB_j:DOC_k)$  represents the AB:DOC aggregate with average initial numbers  $j$  and  $k$  for AB and DOC, respectively. In this picture, the DOC equilibrium is mediated rapidly (probably on the scale of microseconds) via ex-

change between DOC monomers in the bulk and the micelle and aggregates. It is only a semiequilibrium, however, because the AB:DOC aggregates are not in equilibrium with themselves, due to their low solubility, so that the whole system proceeds irreversibly to its final equilibrium state:



The time scale is governed by the flocculation rate of the aggregates (seconds to hours). The solubility, and hence flocculation rate, is expected to depend on  $k/j$  (the DOC:AB molar ratio in the aggregates). Since the differential index of refraction of the supernatant of equilibrium solutions showed that virtually all of the DOC remained in solution (see *Results*),  $k/j$  is expected to decrease with time. The free AB shown in the final equilibrium remains in solution at a very low concentration ( $\sim 10^{-7}$  M).

The facts that the aggregation rates are much slower above the concentration region of DOC micellization and that the DOC:AB ratios are fairly constant suggest that DOC micelles act as a pool of DOC which facilitates the equilibrium exchange of monomers in eq 3 and helps to stabilize the mixed aggregates. The fact that the latter are still unstable even at high DOC concentrations, however, indicates that the low AB solubility is the predominant factor in the behavior of the AB:DOC systems.

## Conclusions

The AB:DOC systems at pH 7.4 are unstable at all concentrations and under the conditions of no added salt and 150 mM NaCl. The rate of flocculation of AB:DOC aggregates increases with decreasing DOC concentration. The instability of AB:DOC systems and their tendency to form large aggregates is in line with the different distribution of both components in the bodies of experimental animals.<sup>33</sup> The compromise between the existing equilibria and the kinetics of aggregation of different AB:carrier (DOC, phospholipids) systems might be related to the different degrees of toxicity of these systems.

## References and Notes

- Medoff, G.; Brajtburg, J.; Kobayashi, G. S.; Bolard, J. *Ann. Rev. Pharmacol. Toxicol.* 1983, 23, 303-330.
- Bolard, J. *Biochim. Biophys. Acta* 1986, 864, 257-304.
- Bennett, J. E.; Hill II, G. J.; Butler, W. T.; Emmons, C. W. *J. Antimicrob. Agents Chemother.* 1963, 745-752.
- Haleblian, J.; McCrone, W. *J. Pharm. Sci.* 1969, 58, 911-929.
- Ghielmetti, G.; Bruzzese, T.; Bianchi, C.; Recusani, F. *J. Pharm. Sci.* 1976, 65, 905-907.
- Forster, D.; Washington, C.; Davis, S. *J. Pharm. Pharmacol.* 1988, 40, 325.
- Mehta, R.; Lopez-Berestein, G.; Hopfer, R.; Mills, K.; Juliano, R. L. *Biochim. Biophys. Acta* 1984, 770, 230-234.
- Szoka, F. C., Jr.; Milholland, D.; Barza, M. *J. Antimicrob. Agents Chemother.* 1987, 31, 421-429.
- Payne, N. I.; Cosgrove, R. F.; Green, A. P.; Liu, L. *J. Pharm. Pharmacol.* 1987, 39, 24-28.
- Janoff, A. S.; Boni, L. T.; Popescu, M. C.; Minchey, S. R.; Cullis, P. R.; Madden, T. D.; Taraschi, T.; Gruner, S. M.; Shyamsunder, E.; Tate, M. W.; Mendelsohn, R.; Bonner, D. *Proc. Natl. Acad. Sci. U.S.A.* 1988, 85, 6122-6126.
- Rinnert, H.; Thirion, C.; Dupont, G.; Lematre, J. *Biopolymers* 1977, 16, 2419-2427.
- Ernst, C.; Grange, J.; Rinnert, H.; Dupont, G.; Lematre, J. *Biopolymers* 1981, 20, 1575-1588.
- Mazerski, J.; Bolard, J.; Borowski, E. *Biochim. Biophys. Acta* 1982, 719, 11-17.
- Lamy-Freund, M. T.; Ferreira, V. F. N.; Schreier, S. *Biochim. Biophys. Acta* 1989, 981, 207-212.
- Lamy-Freund, M. T.; Ferreira, V. F. N.; Schreier, S. *J. Antibiot-*

- ics 1985, 38, 753-757.
16. Lány-Freund, M. T.; Ferreira, V. F. N.; Schreier, S., unpublished results.
  17. Andrews, F. A.; Beggs, W. H.; Sarosi, G. A. *J. Antimicrob. Agents Chemother.* 1977, 11, 615-618.
  18. Andrews, F. A.; Sarosi, G. A.; Beggs, W. H. *J. Antimicrob. Agents Chemother.* 1979, 5, 173-177.
  19. Brajtburg, J.; Elberg, S.; Schwartz, D. R.; Vertut-Croquin, A.; Schlessinger, D.; Kobayashi, G. S.; Medoff, G. *J. Antimicrob. Agents Chemother.* 1985, 27, 172-176.
  20. Sokol-Anderson, M. L.; Brajtburg, J.; Medoff, G. *J. Infect. Dis.* 1986, 154, 76-83.
  21. Reed, C.; Li, X.; Reed, W. F. *Biopolymers* 1989, 28, 1981-2000.
  22. Peitzsch, R. M., M.Sc. Thesis, Tulane University, New Orleans, LA, 1986.
  23. Koppel, D. E. *J. Chem. Phys.* 1972, 57, 4814-4820.
  24. Berne, B.; Pecora, R. *Dynamic Light Scattering*; Wiley: New York, 1976; p 114.
  25. Throughout the paper the data will be expressed in terms of total DOC concentration both for AB:DOC systems and for pure DOC. In AB:DOC systems the mole ratio is 1:2.
  26. Tanford, C. *Physical Chemistry of Macromolecules*; Wiley: New York, 1961; p 287.
  27. Benzonano, G. *Biochim. Biophys. Acta* 1969, 176, 836-848.
  28. Carey, M. C. In *Sterols and Bile Acids*; Danielsson, H.; Sjovall, J., Eds.; Elsevier Science: New York, 1985; pp 345-403.
  29. Small, D. M. *Adv. Chem. Ser.* 1968, 84, 31-52.
  30. Kratochvil, J. P.; Hsu, W. P.; Jacobs, M. A.; Aminabhavi, T. M.; Mukunoki, Y. *Colloid Polym. Sci.* 1983, 261, 781-785.
  31. Kratochvil, J. P.; Hsu, W. P.; Kwok, D. I. *Langmuir* 1986, 2, 256-258.
  32. Kratochvil, J. P. *Hepatology* 1984, 4, 85-97.
  33. Lawrence, R. M.; Hoepflich, P. D.; Jagdia, F. A.; Monji, N.; Huston, A. C.; Schaffner, C. P. *J. Antimicrob. Ther.* 1981, 6, 241-249.

### Acknowledgments

This work was supported by grants from FINEP, CNPq, and FAPESP. M.T.L.F. and S.S. are recipients of CNPq research fellowships. W. Reed is grateful to the Sao Paulo/Interamerican Development Bank Exchange Program for travel support. Partial support from NSF grant DMB-8803760 is also acknowledged.